

Kitaev model on a quantum computer using VQE with Majorana fermions

Ammar Jahin,¹ Andy C. Y. Li,² Thomas Iadecola,^{3,4} Peter P. Orth,^{3,4} Gabriel N. Perdue,² Alexandru Macridin,² M. Sohaib Alam,^{5,6} and Norm M. Tubman⁵

¹*Department of Physics, University of Florida, 2001 Museum Rd, Gainesville, FL 32611, USA*

²*Fermi National Accelerator Laboratory, Batavia, IL, 60510, USA*

³*Department of Physics and Astronomy, Iowa State University, Ames, Iowa 50011, USA*

⁴*Ames Laboratory, Ames, Iowa 50011, USA*

⁵*Quantum Artificial Intelligence Lab. (QuAIL), Exploration Technology Directorate, NASA Ames Research Center, Moffett Field, CA 94035, USA*

⁶*USRA Research Institute for Advanced Computer Science (RIACS), Mountain View, CA, 94043, USA*

(Dated: February 28, 2022)

We study the simulation of the Kitaev spin model on quantum computers. In particular we focus on the models defined on the honeycomb, and square-octagon lattices. Using a fermionic language to describe these models reveals a region of the parameter space that is exactly solvable. We explore an ansatz that is capable of expressing the ground state in the exactly solvable region of the parameter space and extend it outside this region with good accuracy. Doing the calculation using fermions, while requiring the introduction of a non-local map from the fermionic Hilbert space to that of qubits, offers the potentially interesting application of realizing non-abelian anyons on quantum computers, and can also lead to a reduction in the number of qubits required by half.

CONTENTS

I. INTRODUCTION

| | | |
|--------------------------------------------------------------|----|------------------------------------------------------------------------------------------------------------------------------------------------------------------------------------------------------------------------------------------------------------------------------------------------------------------------------------------------------------------------------------------------------------------------------------------------------------------------------------------------------------------------------------------------------------------------------------------------------------------------------------------------------------------------------------------------------------------------------------------------------------------------------------------------------------------------------------------------------------------------------------------------------------------------------------------------------------------------------------------------------------------------------------------------------------------------------------------------------------------------------------------------------------------------------------------------------------------------------------------------------------------------------------------------------------------------------------------------------------------------------------------------------------------------------------------------------------------------------------------------------------------------------------------------------------------------------------------------------------------------------------------------------------|
| I. Introduction | 1 | One of the hallmarks of frustrated interacting two-dimensional quantum spin systems is the emergence of quantum spin liquid ground states with long-range topological order and fractionalized excitations that obey (non-)Abelian statistics [1, 2]. The celebrated Kitaev spin model [3], which describes spins that are interacting on a trivalent lattice via an anisotropic Ising interaction, is a popular playground for theoretically studying such phenomena. Since it is exactly solvable in terms of fermionic operators, many properties of the model can be analytically obtained exactly or within the framework of perturbation theory [3–6]. Kitaev-type exchange interactions are significant in spin-orbit coupled Mott insulators [7] such as the iridium oxide family $A_2\text{IrO}_3$ ($A = \text{Na, Li}$) and $\alpha\text{-RuCl}_3$ [8–11]. This resulted in a flurry of research in the search for an experimental realization of the Kitaev quantum spin liquid [12–14]. These materials exhibit additional interaction terms beyond the Kitaev exchange and show a rich and interesting behavior under an external magnetic field, which cannot be treated easily within the fermionic description and typically requires a numerical analysis. Many numerical studies using various techniques such as exact diagonalization (ED), density-matrix renormalization group (DMRG), and tensor network (TN) methods have revealed new and exotic phases of the model beyond the perturbative regime [7, 15–24]. Effective field theory techniques can also provide valuable insight into the behavior in a magnetic field [25]. |
| II. Kitaev model and fermionic formulation | 2 | |
| A. Kitaev spin Hamiltonian | 2 | |
| B. Representing the model with Majorana fermions | 3 | |
| C. Reducing the Kitaev model to quadratic form | 4 | |
| D. Added interactions | 5 | |
| III. VQE | 5 | |
| A. Fixed-gauge VQE | 5 | |
| 1. Choice of VQE initial state | 5 | |
| 2. Form of variational ansatz | 6 | |
| 3. Simulations and results | 6 | |
| 4. Implications for quantum simulation of non-Abelian anyons | 6 | |
| B. Dynamic gauge VQE | 7 | |
| 1. VQE initial state | 8 | |
| 2. Variational ansatz | 8 | |
| 3. Cost function | 9 | |
| 4. Results | 9 | |
| IV. Conclusion | 9 | |
| Acknowledgments | 10 | |
| A. Relevant parts of the ansatz | 10 | Quantum computers offer an exciting new framework for simulating quantum many-body systems. There are a number of efforts exploring simulation of the Kitaev model on quantum computers [26–28]. In this paper we propose a different way of simulating the model on a quantum computer using a fermionic description. Our motivation is to inject information about the exact solv- |
| B. Mapping the fermionic model onto qubits | 10 | |
| 1. The Jordan-Wigner transformation | 10 | |
| 2. Transforming the Hamiltonian and the ansatz | 11 | |
| References | 12 | |

ability of the model to better treat the problem on the quantum computer. One interesting application of our method is the realization of non-Abelian anyons on quantum computers, which we discuss. The drawback of simulating fermions on quantum computers is the need for a mapping from the fermionic Hilbert space to that of qubits, which necessitates deeper quantum circuits [29–34]. This added circuit depth can make the quantum circuits challenging to run on current noisy intermediate-scale quantum (NISQ) [35] hardware. On the other hand, in certain situations, as will be discussed later, treating the problem using fermions allows for a reduction of the number of qubits by half.

We make use of the variational quantum eigensolver (VQE) [36, 37], a hybrid algorithm (i.e., one using both classical and quantum computers) with significant potential for successful implementation on NISQ devices [36, 38–42]. A VQE algorithm uses a quantum computer to prepare a variational ansatz state, defined using a parameterized quantum circuit, and then measures its energy (i.e., the expectation value of the Hamiltonian in that state). A classical computer is then used to find the optimal set of variational parameters that produces the lowest possible energy expectation value. On a classical computer, preparing the state and calculating the energy expectation value are computationally expensive, so handing these steps over to a quantum computer may offer an effective speed-up. VQE algorithms offer shorter circuits when compared to other methods like adiabatic real-time evolution [43], quantum imaginary time evolution [44], or phase estimation, and thus are viewed as being well-suited for execution on NISQ devices.

The Kitaev spin model with its bond dependent interactions can be defined on any trivalent graph, and in this work we focus on the honeycomb and square-octagon lattices. The exact solution of the model relies on a mapping to a theory of Majorana fermions coupled to a \mathbb{Z}_2 lattice gauge field. In this work, we consider the Kitaev model in the presence of two kinds of additional Hamiltonian terms. First, there are 3-spin interaction terms that do not mix different gauge sectors of the model. These terms allow for the calculation to be restricted to a single gauge sector and lead to a reduction in the number of qubits by half. We also consider external magnetic fields in the x, y , and z -directions, which do mix different gauge sectors together, and in this case we include the full Hilbert space in the calculation.

The rest of the paper is organized as follows. In Sec. II we give a brief review of certain aspects of the Kitaev model that are important for our analysis. Then in Sec. III A we discuss the calculation when restricted to a single gauge sector, and discuss the application of realizing non-Abelian anyons on quantum computers. Finally in Sec. III B we discuss how to extend the calculation to include all gauge sectors of the model.

II. KITAEV MODEL AND FERMIONIC FORMULATION

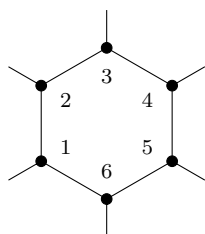
A. Kitaev spin Hamiltonian

A trivalent lattice is one in which every site is connected to three other sites—a condition satisfied, for example, by both the honeycomb and square-octagon lattices as shown in Fig. 1. Throughout the text, we reserve the labels i, j, k, \dots for the lattice sites. The trivalence of the lattice allows for the edges to be split into three disjoint sets, which will be referred to as x, y , and z -edges. The designation of x, y , and z -edges for both the honeycomb and square-octagon lattices is shown in Fig. 1. The Hamiltonian of the Kitaev model is given as,

$$H = - \sum_{\alpha=x,y,z} J_{\alpha} \sum_{\alpha\text{-edges}} \sigma_i^{\alpha} \sigma_j^{\alpha} \quad (1)$$

where σ_i^{α} are Pauli operators at site i and $\alpha = x, y, z$. The summation over edges counts every lattice bond of type α once. Explicitly, on the honeycomb lattice, which has two basis sites $\tau = 1, 2$ per unit cell, it can be written as $H = - \sum_{\alpha} J_{\alpha} \sum_{\mathbf{r}_i} \sigma_{\mathbf{r}_i,1}^{\alpha} \sigma_{\mathbf{r}_i+\delta_{\alpha,2}}^{\alpha}$, where $\mathbf{r}_i = i_1 \mathbf{a}_1 + i_2 \mathbf{a}_2$, and $\delta_x = -\mathbf{a}_1$, $\delta_y = -\mathbf{a}_2$, $\delta_z = 0$. The unit cell vectors \mathbf{a}_i are shown in Fig. 1(a). The square-octagon lattice has four basis sites per unit cell, $\tau = 1, 2, 3, 4$, and its Hamiltonian reads explicitly as $H = - \sum_{\mathbf{r}_i} J_x (\sigma_{\mathbf{r}_i,2}^x \sigma_{\mathbf{r}_i,3}^x + \sigma_{\mathbf{r}_i,4}^x \sigma_{\mathbf{r}_i,1}^x) + J_y (\sigma_{\mathbf{r}_i,1}^y \sigma_{\mathbf{r}_i,2}^y + \sigma_{\mathbf{r}_i,3}^y \sigma_{\mathbf{r}_i,4}^y) + J_z (\sigma_{\mathbf{r}_i,4}^z \sigma_{\mathbf{r}_i+\mathbf{a}_1,2}^z + \sigma_{\mathbf{r}_i,3}^z \sigma_{\mathbf{r}_i+\mathbf{a}_2,1}^z)$. The basis labels τ and unit cell vectors \mathbf{a}_i are shown in Fig. 1(b).

The Kitaev model (1) has a conserved quantity associated with each plaquette p . For the honeycomb lattice there is only one kind of plaquette, and the conserved quantity $[W_p^{(6)}, H] = 0$ takes the form

$$W_p^{(6)} = \sigma_1^x \sigma_2^y \sigma_3^z \sigma_4^x \sigma_5^y \sigma_6^z, \quad (2)$$


For the square-octagon lattice there are two kinds of plaquettes, giving rise to two distinct plaquette operators

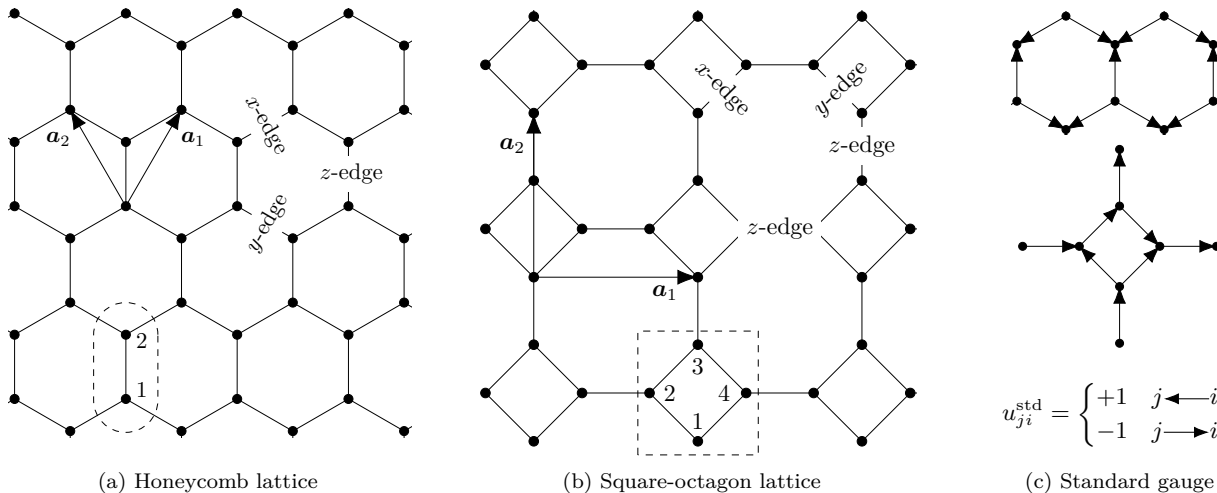
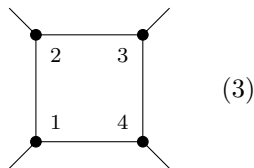


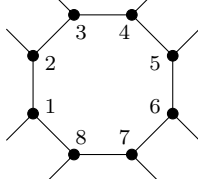
FIG. 1. Different lattices and edge labels. The dashed lines enclose the smallest unit cell of the lattices, and the vectors \mathbf{a}_1 and \mathbf{a}_2 represents the primitive unit vectors.

$$([W_p^{(4)}, H] = [W_p^{(8)}, H] = 0):$$

$$W_p^{(4)} = \sigma_1^z \sigma_2^z \sigma_3^z \sigma_4^z, \quad (3)$$



$$W_p^{(8)} = \sigma_1^x \sigma_2^y \sigma_3^y \sigma_4^x \sigma_5^x \sigma_6^y \sigma_7^y \sigma_8^x, \quad (4)$$



Note that all W_p have eigenvalues of ± 1 since $W_p^2 = 1$. It is useful to decompose the Hilbert space into blocks labeled by the eigenvalues of W_p , i.e., $\mathcal{L} = \bigoplus_w \mathcal{L}_w$, where \mathcal{L} is the full Hilbert space and \mathcal{L}_w denotes the eigenspace corresponding to a particular combination w of eigenvalues of the various W_p operators. A theorem by Lieb [45] tells us that the ground state belongs to the sector with all $W_p = +1$. This sector is referred to as the vortex-free sector.

B. Representing the model with Majorana fermions

The Hilbert space of the lattice is the tensor product of the Hilbert spaces of local spins, $\mathcal{L} = \bigotimes_i \mathcal{L}_i$. We seek a representation of the local spin Hilbert space using 2 fermionic degrees of freedoms at each site, or 4 Majorana fermions. We label this fermionic Hilbert space by $\tilde{\mathcal{L}}_i$. The four Majorana fermions at each site will be labeled as b_i^α , and c_i with $\alpha = x, y, z$. These Majorana operators obey the algebra,

$$\{b_i^\alpha, b_i^\beta\} = 2\delta_{ij}\delta_{\alpha\beta}, \quad \{b_i^\alpha, c_j\} = 0. \quad (5)$$

The 2 dimensional Hilbert space \mathcal{L}_i is the physical subspace of the 4 dimensional Hilbert space $\tilde{\mathcal{L}}_i$. A physical state $|\psi_{\text{phys}}\rangle_i \in \mathcal{L}_i$ is defined such that,

$$D_i |\psi_{\text{phys}}\rangle_i = |\psi_{\text{phys}}\rangle_i, \quad D_i = b_i^x b_i^y b_i^z c_i. \quad (6)$$

The operator D_i acts on the physical subspace as an identity, and since we are only interested in this subspace it should be noted that two operators differing only by factors of D_i are identified in this treatment. Further, given any $|\psi\rangle_i \in \tilde{\mathcal{L}}_i$ the physical part of this state can be extracted as follows,

$$|\psi_{\text{phys}}\rangle_i = \frac{1}{2}(1 + D_i) |\psi\rangle_i. \quad (7)$$

Thus, the operator $1/2(1 + D_i)$ as the local projector operator onto the physical subspace. The full projector can be written as

$$\mathcal{P} = \prod_i \frac{1 + D_i}{2}. \quad (8)$$

In terms of the Majorana fermions, the Pauli operators can take the following form,

$$\sigma_i^x = ib_i^x c_i, \quad \sigma_i^y = ib_i^y c_i, \quad \sigma_i^z = ib_i^z c_i. \quad (9)$$

Using this representation of the Pauli operators the Kitaev model can be written as,

$$H = \sum_\alpha J_\alpha \sum_{\alpha\text{-edges}} i\hat{u}_{ij} c_i c_j, \quad (10)$$

where

$$\hat{u}_{ij} = ib_i^\alpha b_j^\alpha, \quad \hat{u}_{ij}^2 = 1, \quad \hat{u}_{ij} = -\hat{u}_{ji}. \quad (11)$$

Note that the eigenvalues u_{ij} of \hat{u}_{ij} are $u_{ij} = \pm 1$ since $\hat{u}_{ij}^2 = 1$. The operator \hat{u}_{ij} can be interpreted as a

\mathbb{Z}_2 gauge field that couples to the itinerant Majorana fermion c_i . For this reason, we will sometimes refer to the c_i Majorana fermions as “matter” fermions, to distinguish them from the “bond” fermions b_i^α . The operator D_i anticommutes with \hat{u}_{ij} and therefore can be interpreted as implementing a gauge transformation that flips the value of u_{ij} .

C. Reducing the Kitaev model to quadratic form

As noted by Kitaev, the operators \hat{u}_{ij} commute with all terms in the Hamiltonian, so the eigenvalues $u_{ij} = \pm 1$ are conserved quantities of the model. Thus, it is useful to write

$$\tilde{\mathcal{L}} = \bigoplus_u \tilde{\mathcal{L}}_u, \quad (12)$$

where $\tilde{\mathcal{L}}_u$ is the subspace with all u_{ij} specified. The conserved quantities W_p can be expressed in terms of u_{ij} as follows,

$$\begin{aligned} W_p^{(6)} &= \prod_{i \in p} u_{i+1,i}, \\ W_p^{(4)} &= - \prod_{i \in p} u_{i+1,i}, \quad W_p^{(8)} = - \prod_{i \in p} u_{i+1,i} \end{aligned} \quad (13)$$

Thus each subspace $\tilde{\mathcal{L}}_u$ corresponds to a certain configuration of W_p . We will sometimes refer to $\tilde{\mathcal{L}}_u$ as a “gauge sector,” i.e. a sector of the full Hilbert space whose gauge has been fixed by a choice of the eigenvalues u_{ij} .

As noted previously, the ground state belongs to the vortex-free configuration. There are many configurations of u_{ij} that reside in the vortex-free sector. Fig. 1 (c) and (d) define our choice of a “standard configuration” u_{ij}^{std} for both the honeycomb and square-octagon lattices, which is a simple choice of gauge that achieves the vortex-free configuration.

In the subspace $\tilde{\mathcal{L}}_u$, the Hamiltonian in Eq. (10) takes the following quadratic form:

$$H = \frac{i}{2} \sum_{i,j=1}^N K_{ij} c_i c_j, \quad (14)$$

where the matrix $K = u_{ij}$ when i and j make an edge and $K_{ij} = 0$ otherwise. In order to diagonalise a Hamiltonian of this form we need to find a matrix $R \in O(N)$ such that

$$RKR^T = \bigoplus_{n=1}^{N/2} \begin{bmatrix} 0 & \varepsilon_n \\ -\varepsilon_n & 0 \end{bmatrix}, \quad \varepsilon_n \geq 0. \quad (15)$$

This transformation can be achieved by a unitary matrix U ,

$$U^{-1} c_i U = R_{ji} c_j. \quad (16)$$

such that,

$$U^{-1} H U = \frac{i}{2} \sum_{i,j=1}^N [RKR^T]_{ij} c_i c_j \quad (17)$$

$$= i \sum_{n=1}^{N/2} \varepsilon_n c_{2n} c_{2n+1}. \quad (18)$$

To read off the spectrum, it is useful to pair the Majorana fermions into complex fermions. How the Majorana fermions are paired into complex fermion is a matter of basis choice. Here we chose to couple the Majorana fermions inside the same unit cell together. For the honeycomb lattice, the 1 sublattice is coupled to the 2 sublattice, and for the square-octagon lattice, the 1 sublattice is coupled to the 2 sublattice, and the 3 sublattice is coupled to the 4 sublattice. Such a choice of basis can be written in the following way,

$$c_{2n} = a_n + a_n^\dagger, \quad c_{2n+1} = \frac{1}{i}(a_n - a_n^\dagger), \quad (19)$$

$$U^{-1} H U = \sum_n 2\varepsilon_n \left(a_n^\dagger a_n - \frac{1}{2} \right). \quad (20)$$

The ground state of H can be written as $U |\psi_0\rangle$, where

$$a_n |\psi_0\rangle = 0, \quad \text{for all } a_n. \quad (21)$$

The action of the Hamiltonian on $U |\psi_0\rangle$ is found to be,

$$H U |\psi_0\rangle = E_0 U |\psi_0\rangle, \quad (22)$$

$$E_0 = - \sum_{n=1}^{N/2} \varepsilon_n. \quad (23)$$

In designing our VQE ansatz it will be crucial to know what form the operator U takes. A general $SO(N)$ transformation can be applied using $\exp \left[\sum_{ij} \theta_{ij} c_i c_j \right]$, which acts on a Majorana operator c_i as

$$\exp \left[- \sum_{ij} \theta_{ij} c_i c_j \right] c_i \exp \left[\sum_{ij} \theta_{ij} c_i c_j \right] = [e^\theta]_{ji} c_j. \quad (24)$$

Even though any antisymmetric matrix can be brought to the block diagonal form in Eq. (15) by an $SO(N)$ transformation, to ensure that the upper-right element of each block is a positive number (as required) we need to be allowed $O(N)$ transformations. This can be seen as switching the off diagonal elements of a 2×2 matrix is an operation with a determinant of -1 , i.e. σ_x . Thus, we might need to attach a local *particle-hole* transformation to $\exp \left[\sum_{ij} \theta_{ij} c_i c_j \right]$ to make sure all $\varepsilon_n \geq 0$. Note this operation would only be needed if an odd number of the 2×2 block diagonal matrices need such operation. For example, switching the off-diagonal parts of 2 of these 2×2 block-diagonal matrices can be done by a $\sigma_x \oplus \sigma_x$

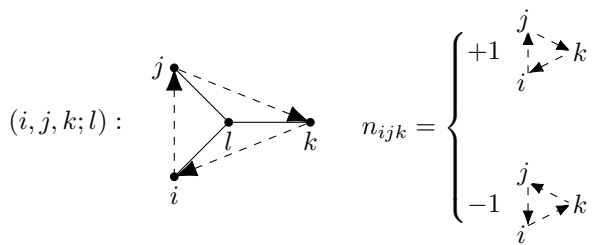


FIG. 2. The definition of the 3-spin terms.

which has a determinant of +1, and is expressible by $\exp\left[\sum_{ij} \theta_{ij} c_i c_j\right]$. In short, it is just the determinant of the transformation that we need to worry about.

This shows that the pure Kitaev model in Eq. (1) is exactly solvable. In the next section we discuss several additional terms of interest that spoil the exact solvability of the model. The form of the exact solution will still be a useful guide when choosing the form of the variational ansatz in the VQE calculation. If we always include U as a part of the ansatz we make sure the algorithm can exactly reproduce the ground state in the exactly solvable limit, where the model is quadratic in terms of fermion operators. We will also add more terms to the ansatz in order to better approximate the ground state in the presence of interactions as we discuss next.

D. Added interactions

Terms added to the Kitaev Hamiltonian fall into two classes: the first class contains terms that do not mix different gauge sectors together, and the second contains terms that do. Here we consider both kinds. This distinction is useful because it informs how the model will be simulated on the quantum computer. For terms of the first kind we only need to simulate a single gauge sector of the model, which is a much smaller Hilbert space than that of the original spin Hilbert space, and may reduce the number of qubits needed for the calculation.

Terms that do not mix different gauge sectors are of the following form,

$$V = - \sum_{(i,j,k;l)} \left[\kappa_a (\sigma_i^x \sigma_j^y \sigma_l^z + \sigma_i^x \sigma_l^y \sigma_k^z + \sigma_l^x \sigma_j^y \sigma_k^z) + \kappa_b \sigma_i^x \sigma_j^y \sigma_k^z \right], \quad (25)$$

where $(i, j, k; l)$, refers to the i, j , and k -th sites connected to the l -th site as shown in Fig. 2. These terms show up at 3rd order when treating an external magnetic field perturbatively. However, we will study the effects of these terms regardless of their origin and treat κ_b and κ_a as independent parameters.

Interestingly, the κ_a and κ_b terms map to very different

looking terms on the fermionic side,

$$V = \sum_{(i,j,k;l)} n_{ijk} \left[i \kappa_a (u_{il} u_{lj} c_j c_i + u_{ik} u_{li} c_i c_k + u_{jl} u_{lk} c_k c_j) + \kappa_b u_{il} u_{jl} u_{kl} c_i c_j c_k c_l \right], \quad (26)$$

where n_{ijk} is defined as in Fig. 2. The κ_a terms do not spoil the exact solvability of the model, and Kitaev showed [3] that they can drive the system into a topologically ordered state. The κ_b terms though, being four-fermion terms, spoil the exact solvability of the model, and their effects are less studied in the literature. Later we discuss one aspect in which these terms can be interesting and useful.

As an example of terms that do mix different gauge sectors, we will consider a uniform external magnetic field,

$$H_{\text{mag}} = - \sum_i [h_x \sigma_i^x + h_y \sigma_i^y + h_z \sigma_i^z]. \quad (27)$$

In the language of the fermionic degrees of freedom this can be written as,

$$H_{\text{mag}} = -i \sum_i [h_x b_i^x c_i + h_y b_i^y c_i + h_z b_i^z c_i]. \quad (28)$$

When simulating the Kitaev model in an external magnetic field, we therefore must include all gauge sectors in the calculation.

III. VQE

A VQE algorithm contains four parts: first, one prepares an initial state $|\psi_0\rangle$, which is typically a state that can be easily prepared on the quantum device. Second, one applies a parameterized unitary (or quantum circuit) $U(\theta)$ with variational parameters θ to the initial state to prepare the ansatz wavefunction $|\psi(\theta)\rangle = U(\theta) |\psi_0\rangle$. The third step is to measure a cost function $C(\theta)$, which is a sum of observables that are being measured in the variational state $|\psi(\theta)\rangle$. To prepare the ground state of a system, the cost function is usually taken to be the energy expectation value $C(\theta) = \langle \psi(\theta) | H | \psi(\theta) \rangle$. However, as we will discuss in the dynamic-gauge VQE section, it can be useful to use a slightly modified cost function. Finally, the fourth step is the classical optimization over the set of parameters θ so as to minimize $C(\theta)$. This involves frequent evaluations of the cost function that follow the first three steps. A VQE algorithm is designed such that the first three steps are carried on a quantum computer while the fourth is done on a classical computer.

A. Fixed-gauge VQE

1. Choice of VQE initial state

Even though the model is most conveniently expressed in terms of Majorana fermions, for the sake of simulating

the system on a quantum computer, we need to group the Majorana fermions into pairs of complex fermions in order to map the problem onto qubits. We already discussed how we choose to group the c_i Majoranas into the complex fermions a_n in Eq. (19), namely,

$$a_n = \frac{1}{2}(c_{2n} + ic_{2n+1}), \quad a_n^\dagger = \frac{1}{2}(c_{2n} - ic_{2n+1}). \quad (29)$$

For the purpose of finding the ground state we choose an initial state in the vortex-free sector of the Hilbert space, where the plaquette operators $W_p^{(\alpha)} = 1$ for all p . Further, we also choose the initial state of the system to be annihilated by all a_n , as defined in Eq. (21).

$$|\psi_0\rangle \in \mathcal{L}_{ustd}, \quad a_n |\psi_0\rangle = 0 \quad \forall a_n. \quad (30)$$

After a Jordan-Wigner transformation, the details of which are discussed in Appendix B, this initial state would simply correspond to the $|0\rangle$ state on the quantum computer, i.e., the all zero state in the Z eigenbasis.

2. Form of variational ansatz

When performing VQE in the fixed-gauge subspace we use an ansatz of the following form:

$$\begin{aligned} |\psi(\boldsymbol{\theta})\rangle &= \exp \left[\sum_{ijkl} \theta_{ijkl}^b c_i c_j c_k c_l \right] \exp \left[\sum_{ij} \theta_{ij}^a c_i c_j \right] |\psi_0\rangle \\ &\equiv U^b(\boldsymbol{\theta}^b) U^a(\boldsymbol{\theta}^a) |\psi_0\rangle \equiv U(\boldsymbol{\theta}) |\psi_0\rangle, \end{aligned} \quad (31)$$

with all components $\boldsymbol{\theta}^a$ and $\boldsymbol{\theta}^b$ being real, and anti-symmetric under the exchange of any two indices. This form of the ansatz is motivated by the Hamiltonian variational ansatz successfully used in quantum chemistry and many-body problems [46, 47]. It contains a unitary single-particle transformation term U^a , which can diagonalize the single-particle sector in the exactly solvable limit, and an interaction term U^b that can account for additional correlations created by four-fermion interaction terms.

We focus on $U^a(\boldsymbol{\theta}^a)$ first. We make this the first part of our ansatz since from our discussion in Sec. IIC, we know it should be capable of expressing the ground state of the pure Kitaev model. For a system with N spins, there are $\frac{N(N-1)}{2}$ independent parameters in $\boldsymbol{\theta}^a$. However, we are not interested in this full set of transformations. Rather we want to mod out the transformations that leave $|\psi_0\rangle$ invariant. We leave the details of such reduction of the ansatz to Appendix A, and give the answer here in terms of the complex fermions a_i defined in Eq. (19),

$$\begin{aligned} U^a(\boldsymbol{\theta}^a) &\equiv \\ \prod_{ij} \exp \left[i\theta_{ij}^{a_1} (a_i^\dagger a_j^\dagger + a_j a_i) \right] \exp \left[\theta_{ij}^{a_2} (a_i^\dagger a_j^\dagger - a_j a_i) \right] \end{aligned} \quad (32)$$

Note that the number of complex fermions for a system described by N Majorana fermions is $N/2$. Thus in total $\boldsymbol{\theta}^a$ contains $\frac{N}{2}(\frac{N}{2} - 1)$ independent parameters.

Recall the discussion below Eq. (24) about the determinant of the transformation needed to diagonalize the Hamiltonian. Since we fix our initial state in Eq. (30), we might need to supplement $U^a(\boldsymbol{\theta}^a)$ with a local *particle-hole* operation, for it to be able to express the ground state. This can easily be done by using $U^a(\boldsymbol{\theta}^a)c_1$ as the ansatz. In all our simulations we compare the optimal energy resulting from using $U^a(\boldsymbol{\theta})$ and $U^a(\boldsymbol{\theta})c_1$, and report the one with lowest energy value.

We also choose not to include all of the quartic terms in $U^b(\boldsymbol{\theta}^b)$ to simplify the circuits used. Though it is not strictly the case, like before, that the dropped terms have no effect on the result, we found that only including the following terms offers the best performance in terms of computation time in our simulations:

$$\begin{aligned} U^b(\boldsymbol{\theta}^b) &\equiv \prod_{nmkl} \exp \left[i\theta_{nmkl}^{b_1} (a_n^\dagger a_m^\dagger a_k^\dagger a_l^\dagger + a_l a_k a_m a_n) \right] \\ &\times \exp \left[\theta_{nmkl}^{b_2} (a_n^\dagger a_m^\dagger a_k^\dagger a_l^\dagger - a_l a_k a_m a_n) \right]. \end{aligned} \quad (33)$$

With that being said, a more careful study of the effect of including the dropped terms might be in order, and we leave this for future work. The number of parameters contained in the above form of $U^b(\boldsymbol{\theta}^b)$ can be found to be $\frac{1}{4!}N(\frac{N}{2} - 1)(\frac{N}{2} - 2)(\frac{N}{2} - 3)$. Thus, the total number of parameters contained in $U(\boldsymbol{\theta})$ is $\frac{N}{2}(\frac{N}{2} - 1) \left[1 + \frac{1}{12}(\frac{N}{2} - 2)(\frac{N}{2} - 3) \right]$. We discuss how to express this ansatz on a quantum computer in Appendix B.

3. Simulations and results

In general, when restricting the Kitaev model with N spins to a single gauge configuration, we end up with N Majorana fermions c_i , one at each site i . This corresponds to $N/2$ complex fermions that we need to simulate, and thus only $N/2$ qubits are needed for computations. This is a substantial reduction compared to simulating the spins directly, which requires N qubits. This reduction makes the fermionic formulations particularly attractive when considering additional terms in the Kitaev model that are ‘‘gauge diagonal’’. Note that the model is no longer exactly solvable when quartic fermion interactions are present, which is where VQE calculations in the fermionic description will be most useful.

We demonstrate the capabilities of the ansatz above using two geometries: a honeycomb lattice with 3×3 unit cells, and a square-octagon lattice with 2×2 unit cells. These geometries have 18 and 16 spins respectively, and thus we only need 9 and 8 qubits for the VQE. Periodic boundary conditions are applied in both cases. We set both models inside the gapless region of the phase diagram. For the honeycomb lattice we set $\vec{J} = (J_x, J_y, J_z) = (1, 1, 1)$, and for the square-octagon

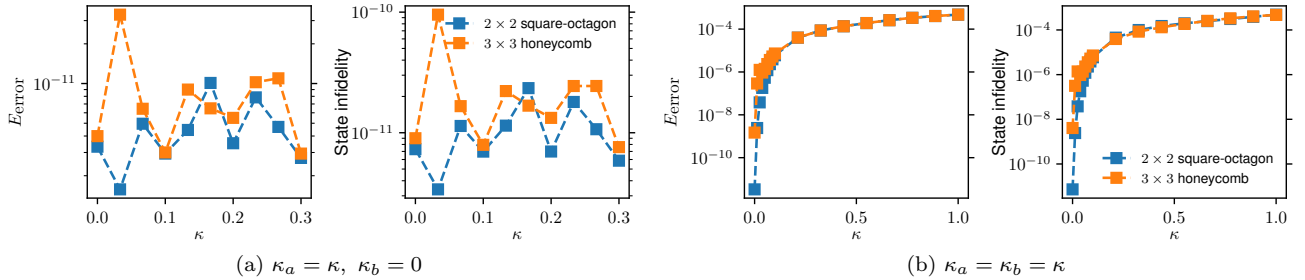


FIG. 3. VQE results for a fixed gauge configuration. Panel (a) is for the exactly solvable quadratic model, while panel (b) includes fermion interactions. The relative error in the energy is defined as $E_{\text{error}} = |(E_{\text{VQE}} - E_{\text{exact}})/E_{\text{exact}}|$, and the state infidelity reads $1 - |\langle \psi_{\text{exact}} | \psi_{\text{VQE}} \rangle|^2$. The results shown that the ansatz does what it was set out to do. It is capable of reproducing the ground state in the exactly solvable cases. The accuracy of the model ranges from 10^{-10} to 10^{-4} depending on how strong the interaction terms κ_b are. Our method here has the advantage of cutting the number of qubits needed by half when compared to simulating the model directly from the spins on the lattice.

lattice we set $\vec{J} = (1, 1, \sqrt{2})$. Further, we test the ansatz for the cases of $\kappa_a = \kappa$, $\kappa_b = 0$, and $\kappa_a = \kappa_b = \kappa$. The results are shown in Fig. 3. As expected, for the case $\kappa_b = 0$ the optimized ground state shows excellent agreement with the exact ground state found by exact diagonalization. Also, as expected, when moving away from the exactly solvable limit, we see a noticeable decrease in the accuracy of the ansatz. However, it is worth mentioning that the accuracy is comparable to other ansatzes in the literature treating the model from the spin language directly [26, 27].

4. Implications for quantum simulation of non-Abelian anyons

A potentially interesting application for our method is realizing non-Abelian anyons on quantum computers. Let us for now focus on the honeycomb lattice, though the square-octagon case is not substantially different. With $\vec{J} = (1, 1, 1)$ and $\kappa_a = \kappa_b = 0$, the model is gapless. Adding the κ_a terms opens up a gap in the spectrum. One of the interesting features of the model in this region of the parameter space is that it hosts non-Abelian anyons [3]. In particular, a vortex excitation of the model (i.e., a plaquette p for which $W_p = -1$) will carry a Majorana zero mode. One can therefore imagine using VQE methods to prepare the ground state in the presence of some number of vortices. Then, by applying appropriate unitary transformations to this state (see, e.g., [48]), one could manipulate the vortices in order to “braid” the attached Majorana zero modes, which is one route to realizing fault-tolerant Clifford operations [49]. We discuss below some considerations that must be taken into account when contemplating such a scheme.

If we have an infinite system with two vortices that are very far from each other, we expect two degenerate ground states that have the same energy and different fermion parity. In both classical and quantum simulations, we only have access to finite systems and there is

a limit to how far away the vortices can be from each other. As the Majorana modes get close to each other they can hybridize, leading to a small energy gap between the even- and odd-parity states. We henceforth refer to this energy scale as the “ground-state splitting,” to avoid confusion with the (larger) energy scale of the bulk gap. In practice, it is desirable for this splitting to be as small as possible to suppress the accumulation of dynamical phases during braiding. The degree of closeness between the Majorana zero modes can be quantified by comparing the distance between the vortices to the correlation length ξ . It is thus desirable to make ξ as small as possible, so that the vortices do not need to be very far apart during braiding. For $\kappa_a \ll |\vec{J}|$, one can show that $\xi \propto 1/\kappa_a$. However, we also expect this behavior to change for large κ_a , since a theory with only κ_a terms (without J_x , J_y and J_z terms) will be gapless, and thus has $\xi = \infty$. We thus expect the ξ to have a minimum value as a function of κ_a . This minimum value of ξ is crucial since it puts a lower bound on the system sizes where we expect to observe the topological properties of the model.

For instance, to have robust Majorana modes on a quantum computer we have to be able to simulate systems whose sizes are of the order of 2ξ for periodic boundary conditions. (Having open boundaries would not help since we will also need to require the Majorana modes to be away from the boundary.) Thus the lower bound on ξ also puts a lower bound on the system sizes where we expect to see robust Majorana modes using only the κ_a terms. This is one area where we find that including the κ_b terms can be of some help, as we will now explain.

Two Majorana modes can fuse into either the vacuum or a fermion, with both states having the same energy, making a gapless system. However, if the two Majorana modes are close to each other, they can hybridize and open up a gap. Thus, a proxy for how robust two Majorana modes are in our system can be the energy gap in the presence of the Majorana modes, which we calculate in Fig. 4 as a function of κ_a for a 3×3 honeycomb

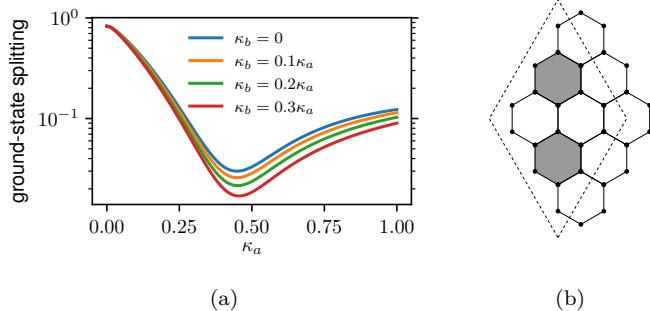


FIG. 4. (a) The energy splitting between the ground and the first excited states on a 3×3 honeycomb lattice with two vortices present (shown in gray) in panel (b). Each vortex hosts a Majorana fermion, and in the limit where the vortices are infinitely separated we expect a doubly degenerate ground state manifold. However, because of the finite size of our sample, the two states hybridize, and there is a splitting in energy. This splitting in energy would spoil the study of braiding properties of the vortices. How big the splitting will depend on a correlation length. The correlation length is bounded from below when we only consider κ_a terms. However, when adding the κ_b terms we can lower the splitting more.

lattice with periodic boundary conditions. Indeed we notice that the gap follows a similar trend to that expected for the correlation length ξ and is bounded from below. However, we find that the gap can be further lowered by adding the κ_b terms. This can be crucial when the calculation is limited in the number of qubits that can be used, but we still want to make the Majorana modes more robust.

B. Dynamic gauge VQE

1. VQE initial state

In this section, we consider the case of arbitrary nonzero external magnetic fields. In this case, one can no longer restrict the calculation to only one of the $\tilde{\mathcal{L}}_u$ subspaces, where the configuration of fluxes W_p [see Eq. (13)] is fixed. This follows from Eq. (28), where the $ib_i^\alpha c_i$ terms flip the sign of the u_{ij} bond variable with $(i, j) \in \alpha$ -edges. We thus need to consider the full fermionic Hilbert space $\tilde{\mathcal{L}} = \bigoplus_u \tilde{\mathcal{L}}_u$, which includes all flux sectors. To map the system onto qubits, we note that each link variable u_{ij} can be represented by a single qubit. A system of N spins thus requires $2N$ qubits to simulate both the flux degrees of freedom and the fermionic (matter) subspace.

In the last section we discussed how to group the c_i (matter) Majorana fermions into complex fermions, see Eq. 19. Similarly, the b_i^α (bond) Majorana fermions can be combined into complex fermions in the following way,

$$g_{(i,j)} = \frac{1}{2}(b_i^\alpha + ib_j^\alpha), \quad g_{(i,j)}^\dagger = \frac{1}{2}(b_i^\alpha - ib_j^\alpha), \quad (34)$$

where $\alpha = x, y, z$ depending whether $(i, j) \in x, y, z$ -edges. Using this basis we can write the gauge variables as

$$\hat{u}_{ij} = ib_i^\alpha b_j^\alpha = 2g_{(i,j)}^\dagger g_{(i,j)} - 1, \quad (35)$$

and thus initializing a state in a specific gauge configuration amounts to choosing whether a certain fermionic orbital is occupied or empty.

In the same way as we label the sites of the model with Latin indices i, j, k, \dots , we will label the edges using Greek letters μ, ν, λ, \dots . However there is an ambiguity when writing g_μ for example since $g_{(i,j)} \neq g_{(j,i)}$, but (i, j) and (j, i) are the same edge. In order to remove this ambiguity we define g_ν such that $g_\nu^\dagger g_\nu = 1$ on all edges corresponds to the standard configuration u_{ij}^{std} .

We choose to initialize the system in the standard gauge configuration, with all $u_{ij} = 1$. Thus our initial state is such that

$$g_\nu^\dagger |\psi_0\rangle = 0, \quad \forall g_\nu^\dagger \quad (36)$$

2. Variational ansatz

The ansatz we use for the calculation in the full Hilbert space reads

$$\begin{aligned} |\psi(\boldsymbol{\theta})\rangle &= \exp\left[\sum \theta_{ij}^c c_i b_j\right] \exp\left[\sum \theta_{ij}^b b_i b_j\right] \\ &\quad \times \exp\left[\sum \theta_{ij}^a c_i c_j\right] |\psi_0\rangle \\ &\equiv U^c(\boldsymbol{\theta}^c) U^b(\boldsymbol{\theta}^b) U^a(\boldsymbol{\theta}^a) |\psi_0\rangle. \end{aligned} \quad (37)$$

Similarly to the discussion in Sec. III A 2, and Appendix A, we choose to reduce the number of parameters by keeping only the following terms,

$$\begin{aligned} U^a(\boldsymbol{\theta}^a) &= \\ \exp\left[\sum_{nm} \left[i\theta_{nm}^{a1} (a_n^\dagger a_m^\dagger + a_m a_n) + \theta_{nm}^{a2} (a_n^\dagger a_m^\dagger - a_m a_n) \right]\right], \end{aligned} \quad (38)$$

$$\begin{aligned} U^b(\boldsymbol{\theta}^b) &= \\ \exp\left[\sum_{\mu\nu} \left[i\theta_{\mu\nu}^{b1} (g_\mu^\dagger g_\nu^\dagger + g_\nu g_\mu) + \theta_{\mu\nu}^{b2} (g_\mu^\dagger g_\nu^\dagger - g_\nu g_\mu) \right]\right], \end{aligned} \quad (39)$$

$$\begin{aligned} U^c(\boldsymbol{\theta}^c) &= \\ \exp\left[\sum_{m\mu} \left[i\theta_{m\mu}^{c1} (a_m^\dagger g_\mu^\dagger + g_\mu a_m) + \theta_{m\mu}^{c2} (a_m^\dagger g_\mu^\dagger - g_\mu a_m) \right]\right]. \end{aligned} \quad (40)$$

Here, $\boldsymbol{\theta}^a$ contains $\frac{N}{2}(\frac{N}{2}-1)$ parameters for a system with N spins. Such a system will have $\frac{3N}{2}$ edges, and thus $\boldsymbol{\theta}^b$ contains $\frac{3N}{2}(\frac{3N}{2}-1)$ parameters, and $\boldsymbol{\theta}^c$ contains $\frac{3N^2}{2}$ parameters. In total, the ansatz $U(\boldsymbol{\theta})$ has $2N(2N-1)$ parameters.

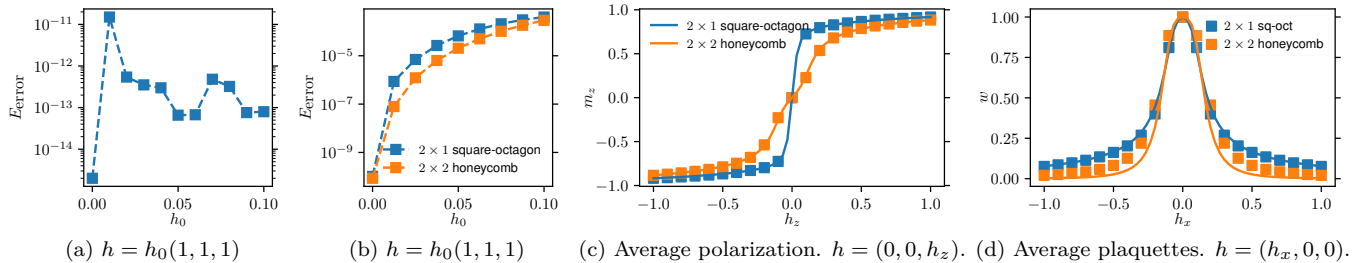


FIG. 5. Dynamic gauge VQE results. Panels (a) and (b) show the error in energy comparing the VQE results to exact diagonalization, $E_{\text{error}} = |(E_{\text{VQE}} - E_{\text{exact}})/E_{\text{exact}}|$. Panel (c) shows that an external field induces a finite magnetization that is saturating when the field becomes of the order of the Kitaev exchange. Panel (d) shows the proliferation of fluxes induced by an external field. This gives a quantitative estimate on the extent of the perturbative regime, where one considers only the flux free sector with $w = 1$. The system starts out from the gapless point for zero field. Solid lines are exact, and the squares are from the optimal VQE state.

3. Cost function

The variational state in Eq. 37 explores states in the full Hilbert space, which includes both physical and unphysical states. When using the expectation value of the energy $C(\theta) = \langle \psi(\theta) | H | \psi(\theta) \rangle$ as a cost function, it is not guaranteed that the optimal state $\psi(\theta_{\text{optimal}})$ belongs to the physical subspace. Unphysical states are defined such that $\mathcal{P}|\psi\rangle = 0$, where \mathcal{P} is the projection operator as defined in Eq. (8). Therefore, we use the following cost function

$$C(\theta) = \frac{\langle \psi(\theta) | \mathcal{P} H | \psi(\theta) \rangle}{\langle \psi(\theta) | \mathcal{P} | \psi(\theta) \rangle}, \quad (41)$$

which explicitly includes the projector onto the physical subspace. We observed that using this cost function, the algorithm always converged to a physical state in all the cases tested.

In Appendix B we discuss the Jordan-Wigner transformation of the Majorana fermions of the Kitaev model. The Jordan-Wigner transformation of the projection operator \mathcal{P} (much like the Hamiltonian) is a sum of Pauli strings. Since both \mathcal{P} and H are a sum of Pauli strings, $\mathcal{P}H$ is also a sum of Pauli strings. Pauli strings are observables that can be measured on a quantum computer, and how to measure sum of Pauli strings efficiently has been discussed in the literature [50–54].

4. Results

With the gauge variables being dynamic, we demonstrate the capabilities of the ansatz above using three geometries: 1×1 square-octagon, 2×1 square-octagon, and 2×2 honeycomb lattice. These geometries have 4, 8 and 8 spins, respectively, and thus require 8, 16, and 16 qubits in the simulation. Periodic boundary conditions are applied in both cases. As before, we set both models inside the gapless region of the phase diagram. For the honeycomb lattice we set $J = (1, 1, 1)$, and for the

square-octagon lattice we set $J = (1, 1, \sqrt{2})$. Fig. 5 (a) and (b) show the error in the ground state energy comparing the VQE results to that of exact diagonalization for $\mathbf{H} = h_0(1, 1, 1)$. Adding the magnetic field terms does not change the fact that the model is invariant under a gauge transformation. Thus the full fermionic Hilbert space has many degenerate ground states that can be related to each other by a gauge transformation. This makes comparing state fidelity a lot harder than in the fixed VQE case, especially for the 16 qubit cases where getting the full spectrum using exact diagonalization is time consuming and we had to resort to only solving for the ground state even classically. There is no guarantee that the ground state found by exact diagonalization should be the same as the ground state found by the VQE algorithm. We do expect them to be gauge related, though. In Fig. 5 (c) and (d) we show the average polarization and average number of plaquettes respectively. These are two gauge independent quantities that should be equal between the ground state obtained by exact diagonalization and our variational ground state. Both quantities agree pretty well between the exact diagonalization ground state and our VQE ground state.

IV. CONCLUSION

We use the variational quantum eigensolver (VQE) method to simulate ground state properties of Kitaev spin models on the honeycomb and square-octagon lattices. Following Kitaev’s original decomposition of spins into fermions, we simulate a fermionic description of the model. We show that this can reduce the number of required qubits by a factor of two, if one can restrict states to a fixed gauge sector. We present results for systems up to 18 spins and show that VQE can find the ground state with high accuracy not only in the exactly solvable limit, but also in the presence of additional gauge-diagonal terms that render the fermionic matter sector interacting. Such terms arise, for example, when treat-

ing external magnetic fields within perturbation theory and can drive the system into a non-Abelian topological phase. We highlight the potential application of our method in realizing non-Abelian anyons on quantum computers. We also perform VQE simulations in the presence of terms that couple different gauge sectors, in which case one requires $2N$ qubits to simulate N spins, restricting the maximal system sizes we can reach to $N = 8$. We show results for the magnetization and the average number of fluxes induced by an external field that agree well results from exact diagonalization. Our results compare well to other VQE results of the model in the literature, and demonstrate that fermionizing spin models can provide an advantage when additional constraints limit the size of the Hilbert space where the ground state is located.

ACKNOWLEDGMENTS

This material is based upon work supported by the U.S. Department of Energy, Office of Science, National Quantum Information Science Research Centers, Superconducting Quantum Materials and Systems Center (SQMS) under the contract No. DE-AC02-07CH11359. We would like to thank the entire SQMS algorithms team for fruitful and thought provoking discussions around this work.

Appendix A: Relevant parts of the ansatz

Our ansatz introduced in Sec. III A 2 can be simplified by modding out the parts of the ansatz that leaves the initial state invariant. Let us look at the action of $U^a(\theta^a)$ on $|\psi_0\rangle$, where

$$U^a(\theta^a) = \exp \left[\sum_{ij} \theta_{ij}^a c_i c_j \right], \quad (\text{A1})$$

and $a_i |\psi_0\rangle = 0$ for all a_i . We begin by writing $U^a(\theta^a)$ in terms of the complex fermions a_i ,

$$\begin{aligned} U^a(\theta^a) &= \exp \sum_{ij} (\theta_{2i,2j}^a c_{2i} c_{2j} + \theta_{2i+1,2j}^a c_{2i+1} c_{2j} \\ &\quad + \theta_{2i,2j+1}^a c_{2i} c_{2j+1} + \theta_{2i+1,2i+1}^a c_{2i+1} c_{2j+1}) \\ &= \exp \left[\sum_{ij} \left[i\theta_{ij}^{a1} (a_i^\dagger a_j + a_j^\dagger a_i) + \theta_{ij}^{a2} (a_i^\dagger a_j - a_j^\dagger a_i) \right] \right. \\ &\quad \left. + \sum_{ij} \left[i\theta_{ij}^{a3} (a_i^\dagger a_j^\dagger + a_j a_i) + \theta_{ij}^{a4} (a_i^\dagger a_j^\dagger - a_j a_i) \right] \right], \quad (\text{A2}) \end{aligned}$$

where it can be shown that,

$$\begin{aligned} \theta_{ij}^{a1} &= \theta_{2i,2j}^a - \theta_{2i+1,2j+1}^a \\ \theta_{ij}^{a2} &= \theta_{2i,2j}^a + \theta_{2i+1,2j+1}^a \\ \theta_{ij}^{a3} &= \theta_{2i+1,2j}^a + \theta_{2i,2j+1}^a \\ \theta_{ij}^{a4} &= \theta_{2i+1,2j}^a - \theta_{2i,2j+1}^a \end{aligned} \quad (\text{A3})$$

Since the commutators $[a_i^\dagger a_j, a_i^\dagger a_{j'}]$, $[a_i^\dagger a_j, a_i a_{j'}]$, $[a_i^\dagger a_j^\dagger, a_i a_{j'}]$, and $[a_i a_j, a_i a_{j'}]$ are either zero or a quadratic product of a_i 's and a_i^\dagger 's we can write

$$\begin{aligned} &\exp \left[\sum_{ij} \left[i\theta_{ij}^{a3} (a_i^\dagger a_j + a_j^\dagger a_i) + \theta_{ij}^{a4} (a_i^\dagger a_j - a_j^\dagger a_i) \right] \right. \\ &\quad \left. + \sum_{ij} \left[i\theta_{ij}^{a1} (a_i^\dagger a_j^\dagger + a_j a_i) + \theta_{ij}^{a2} (a_i^\dagger a_j^\dagger - a_j a_i) \right] \right] \\ &= \prod_{ij} \exp \left[i\theta_{ij}^{a1} (a_i^\dagger a_j^\dagger + a_j a_i) \right] \exp \left[\theta_{ij}^{a2} (a_i^\dagger a_j^\dagger - a_j a_i) \right] \\ &\times \prod_{ij} \exp \left[i\theta_{ij}^{a3} (a_i^\dagger a_j + a_j^\dagger a_i) \right] \exp \left[\theta_{ij}^{a4} (a_i^\dagger a_j - a_j^\dagger a_i) \right] \end{aligned} \quad (\text{A4})$$

However since the parameters in the exponent are to be found variationally anyway, the exact relationship between the primed and unprimed θ 's is not relevant, and we can just as well use the RHS of the equation above in our ansatz. Finally we notice that,

$$\begin{aligned} &\prod_{ij} \exp \left[i\theta_{ij}^{a3} (a_i^\dagger a_j + a_j^\dagger a_i) \right] \exp \left[\theta_{ij}^{a4} (a_i^\dagger a_j - a_j^\dagger a_i) \right] |\psi_0\rangle \\ &= e^{i\phi} |\psi_0\rangle \end{aligned} \quad (\text{A5})$$

since $a_i |\psi_0\rangle = 0$ for all a_i . Thus in our ansatz we only use

$$\begin{aligned} U^a(\theta^a) &\equiv \\ &\prod_{ij} \exp \left[i\theta_{ij}^{a1} (a_i^\dagger a_j^\dagger + a_j a_i) \right] \exp \left[\theta_{ij}^{a2} (a_i^\dagger a_j^\dagger - a_j a_i) \right] \end{aligned} \quad (\text{A6})$$

without any loss of generality. For a system with N spins, the above expression has $N/2(N/2-1)$ as opposed to the $N(N-1)/2$ independent parameters of Eq. (A1).

Appendix B: Mapping the fermionic model onto qubits

1. The Jordan-Wigner transformation

Consider a fermionic Hilbert space of N orbitals (we take orbital here to also include the spin) with a_i , $i \in \{1, \dots, N\}$ being the annihilation operators for these N orbitals. This Hilbert space is 2^N dimensional, since each

orbital can either be full or empty. The operators a_i 's satisfy the following anti-commutation relationships,

$$\{a_i, a_j^\dagger\} = \delta_{ij}, \quad \{a_i, a_j\} = 0. \quad (\text{B1})$$

A basis of this Hilbert space can be defined as

$$|n_1 \dots n_N\rangle = (a_1^\dagger)^{n_1} \dots (a_N^\dagger)^{n_N} |0\rangle, \quad n_i \in \{0, 1\}, \quad (\text{B2})$$

where $|0\rangle$ is the state annihilated by all lowering operators. The lowering operators has the following action on the basis states,

$$a_i |n_1 \dots n_i \dots n_N\rangle = \begin{cases} 0, & n_i = 0, \\ \xi_i |n_1 \dots 0 \dots n_N\rangle, & n_i = 1, \end{cases} \quad (\text{B3})$$

where

$$\xi_i = (-1)^{\sum_{j<i} n_j} \quad (\text{B4})$$

is the parity counting of all the fermions with a labels $j < i$. This phase factor is what makes mapping a system of fermions on a system of bosons not very straight forward. The definition of our basis states depends (up to a sign) on how we choose to order the orbitals.

A system of N qubits has a Hilbert space that is spanned by,

$$|s_1 \dots s_N\rangle = (\sigma_1^+)^{s_1} \dots (\sigma_N^+)^{s_N} |0\rangle, \quad s_i \in \{0, 1\}, \quad (\text{B5})$$

where $\sigma_i^+ = \frac{1}{2}(\sigma_i^x - i\sigma_i^y)$, and the state $|0\rangle$ is defined such that $\sigma_i^- |0\rangle = 0$ for all $\sigma_i^- = (\sigma_i^+)^{\dagger}$. This Hilbert space is also 2^N dimensional and it looks very similar to the fermionic system. We can try and make the identifications $\sigma_i^- = a_i$, and $\sigma_i^+ = a_i^\dagger$. However there is an important difference, the action of σ_i^- on the basis states does not include the parity counting phase,

$$\sigma_i^- |s_1 \dots s_i \dots s_N\rangle = \begin{cases} 0, & s_i = 0, \\ |s_1 \dots 0 \dots s_N\rangle, & s_i = 1. \end{cases} \quad (\text{B6})$$

The Jordan-Wigner mapping then seek to restore this parity counting phase by making the following identifications,

$$a_i = \prod_{j<i} \sigma_j^z \sigma_i^-, \quad a_i^\dagger = \prod_{j<i} \sigma_j^z \sigma_i^+. \quad (\text{B7})$$

2. Transforming the Hamiltonian and the ansatz

As discussed in the main text, it is useful to have a distinction between two kinds of Majoranas of the Kitaev model, the b_i^α Majoranas that make up the gauge sector and the c Majoranas that make up the fermionic sector. In the main text we chose to have,

$$c_{2n} = a_n + a_n^\dagger, \quad c_{2n+1} = \frac{1}{i}(a_n - a_n^\dagger). \quad (\text{B8})$$

Since a pair of Majoranas combine to make a complex fermion, for a system of N spins the index n above ranges from 1 to $N/2$. Using the transformation in Eq. (B7) we see that the Majorana fermions maps to the following,

$$c_{2n} = \prod_{m<n} \sigma_m^z \sigma_n^x \quad c_{2n+1} = \prod_{m<n} \sigma_m^z \sigma_n^y. \quad (\text{B9})$$

Further, we also have a complex fermion g_μ associated with each edge as discussed in the main text. Since the complex fermions g_μ are defined in such a specific way such that $g_\mu^\dagger g_\mu = 1$ corresponds to the standard gauge configuration u_{ij}^{std} , we need a new notation for the b_i^α Majorana fermions in order to avoid ambiguous notations and properly keep track of minus signs. We define,

$$b_\nu^1 = g_\nu^\dagger + g_\nu \quad b_\nu^2 = \frac{1}{i}(g_\nu^\dagger - g_\nu), \quad (\text{B10})$$

For the Jordan-Wigner transformation we make the following identification,

$$g_\nu \equiv a_{\nu+N/2}. \quad (\text{B11})$$

With this we can extend the Jordan-Wigner transformation to include the b_i^α Majorana Fermions

$$b_\nu^1 = \prod_{m<\nu+N/2} \sigma_m^z \sigma_{\nu+N/2}^x \quad b_\nu^2 = \prod_{m<\nu+N/2} \sigma_m^z \sigma_{\nu+N/2}^y. \quad (\text{B12})$$

Using Eqs. (B9) and (B12) one can work out the Jordan-Wigner transformation of all possible terms in the Hamiltonian. Defining

$$S_{ji} = \prod_{j<p<i} \sigma_p^z \quad (\text{B13})$$

the fixed gauge Hamiltonian transforms as follows,

$$\sum_{j>i} iA_{ij} c_i c_j = \sum_{j>i} A_{ij} i\sigma_{i'}^{\alpha_i} S_{i'j'} \sigma_{j'}^{\alpha_j}, \quad (\text{B14})$$

$$\sum_{l>k>j>i} V_{ijkl} c_i c_j c_k c_l = \sum_{l>k>j>i} \sigma_{i'}^{\alpha_i} S_{i'j'} \sigma_{j'}^{\alpha_j} \sigma_{k'}^{\alpha_k} S_{k'l'} \sigma_{l'}^{\alpha_l}, \quad (\text{B15})$$

with $i', j', k', l' = \lfloor i/2 \rfloor, \lfloor j/2 \rfloor, \lfloor k/2 \rfloor, \lfloor l/2 \rfloor$, $\alpha_i = x$ when i is even, and $\alpha_i = y$ when i is odd.

When dealing with dynamic gauge Hamiltonian we have,

$$\sum_{j>i} J_\alpha c_i c_j b_i^\alpha b_j^\alpha = i\sigma_{i'}^{\alpha_i} S_{i'j'} \sigma_{j'}^{\alpha_j} \left[s_{ij} \sigma_{\nu+N/2}^z \right], \quad (\text{B16})$$

$$\sum_i h_\alpha c_i b_i^\alpha = i\sigma_{i'}^{\alpha_i} S_{i'\nu+N/2} \sigma_{\nu+N/2}^{\beta_\alpha} \quad (\text{B17})$$

where $s_{ij} = \pm 1$, and $\beta_\alpha = x, y$ when $b_i^\alpha = b_\nu^1$, or $b_i^\alpha = b_\nu^2$ respectively.

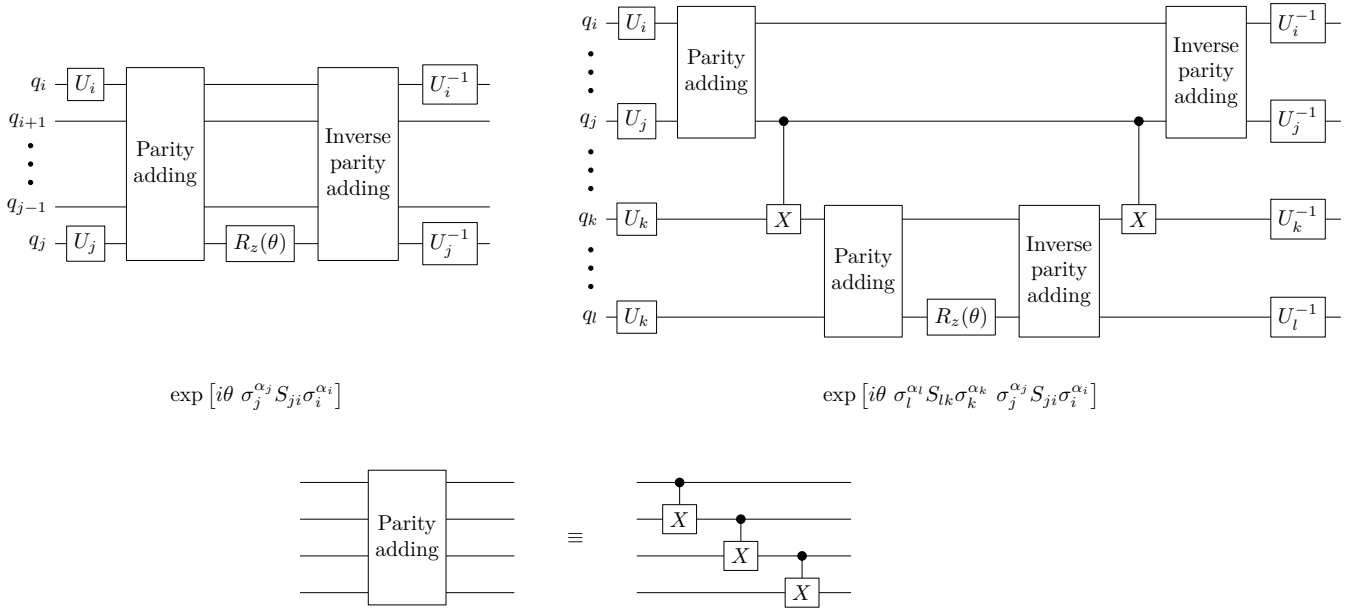


FIG. 6. Building blocks for the ansatz. Here $U_i = H$ (Hadamard gate) if $\alpha_i = x$, and $U_i = R_x(\frac{\pi}{2})$ (rotation about x -axis by $\pi/2$) if $\alpha_i = y$.

We now move on to the Jordan-Wigner transformed ansatz. We start with

$$U^a(\theta^a) \equiv \prod_{i < j} \exp [i\theta_{ij}^{a1} (a_i^\dagger a_j^\dagger + a_j a_i)] \exp [\theta_{ij}^{a2} (a_i^\dagger a_j^\dagger - a_j a_i)]. \quad (\text{B18})$$

Using Eq. B7, we can write the exponents as

$$a_i^\dagger a_j^\dagger + a_j a_i = 2(\sigma_i^x S_{ij} \sigma_j^x - \sigma_i^y S_{ij} \sigma_j^y) \quad (\text{B19})$$

$$a_i^\dagger a_j^\dagger - a_j a_i = -2i(\sigma_i^x S_{ij} \sigma_j^y + \sigma_i^y S_{ij} \sigma_j^x) \quad (\text{B20})$$

Next we look into the transformation of

$$U^b(\theta^b) \equiv \prod_{i < j < k < l} \exp [i\theta_{ijkl}^{b1} (a_i^\dagger a_j^\dagger a_k^\dagger a_l^\dagger + a_l a_k a_j a_i)] \times \exp [\theta_{ijkl}^{b2} (a_i^\dagger a_j^\dagger a_k^\dagger a_l^\dagger - a_l a_k a_j a_i)]. \quad (\text{B21})$$

Using Eq. B7 the exponents can be transformed as follows,

$$a_n^\dagger a_m^\dagger a_k^\dagger a_l^\dagger + a_l a_k a_m a_n = (\sigma_i^x S_{ij} \sigma_j^x \sigma_k^x S_{kl} \sigma_l^x - \sigma_i^y S_{ij} \sigma_j^y \sigma_k^x S_{kl} \sigma_l^x - \text{all permutations of } x, y + \sigma_i^y S_{ij} \sigma_j^y \sigma_k^y S_{kl} \sigma_l^y) \quad (\text{B22})$$

$$a_n^\dagger a_m^\dagger a_k^\dagger a_l^\dagger - a_l a_k a_m a_n = 2i (\sigma_i^y S_{ij} \sigma_j^y \sigma_k^y S_{kl} \sigma_l^x + \text{all permutations of } x, y - \sigma_i^x S_{ij} \sigma_j^x \sigma_k^x S_{kl} \sigma_l^y + \text{all permutations of } x, y). \quad (\text{B23})$$

In Fig. 6 we show how this transformed ansatz can be implemented on a quantum computer. Finally, we note that the ansatz used in the dynamical gauge VQE (Eqs. (38, 39, 40)) can be transformed to operators that can be acted with on qubits using equations that are very similar to Eqs. (B19) and (B20).

-
- [1] L. Balents, *Nature* **464**, 199 (2010).
 [2] L. Savary and L. Balents, *Reports on Progress in Physics* **80**, 016502 (2017).
 [3] A. Kitaev, *Annals of Physics* **321**, 2–111 (2006).
 [4] S. Yang, D. L. Zhou, and C. P. Sun, *Physical Review B*

- 76**, 180404 (2007).
 [5] G. Baskaran, S. Mandal, and R. Shankar, *Phys. Rev. Lett.* **98**, 247201 (2007).
 [6] M. Hermanns, I. Kimchi, and J. Knolle, *Annu. Rev. Cond. Mat. Phys.* **9**, 17 (2018).

- [7] J. c. v. Chaloupka, G. Jackeli, and G. Khaliullin, *Phys. Rev. Lett.* **105**, 027204 (2010).
- [8] J. Chaloupka, G. Jackeli, and G. Khaliullin, *Phys. Rev. Lett.* **105**, 027204 (2010).
- [9] J. G. Rau, E. K.-H. Lee, and H.-Y. Kee, *Annual Review of Condensed Matter Physics* **7**, 195 (2016).
- [10] K. W. Plumb, J. P. Clancy, L. J. Sandilands, V. V. Shankar, Y. F. Hu, K. S. Burch, H.-Y. Kee, and Y.-J. Kim, *Phys. Rev. B* **90**, 041112 (2014).
- [11] H. Takagi, T. Takayama, G. Jackeli, G. Khaliullin, and S. E. Nagler, *Nature Reviews Physics* **1**, 264 (2019).
- [12] A. Banerjee, C. A. Bridges, J.-Q. Yan, A. A. Aczel, L. Li, M. B. Stone, G. E. Granroth, M. D. Lumsden, Y. Yiu, J. Knolle, S. Bhattacharjee, D. L. Kovrizhin, R. Moessner, D. A. Tennant, D. G. Mandrus, and S. E. Nagler, *Nat. Mater.* **advance online publication** (2016).
- [13] N. Janša, A. Zorko, M. Gomilšek, M. Pregelj, K. W. Krämer, D. Biner, A. Biffin, C. Rüegg, and M. Klanjšek, *Nature Phys* **14**, 786 (2018).
- [14] Y. Kasahara, T. Ohnishi, Y. Mizukami, O. Tanaka, S. Ma, K. Sugii, N. Kurita, H. Tanaka, J. Nasu, Y. Motome, T. Shibauchi, and Y. Matsuda, *Nature* **559**, 227 (2018).
- [15] C. Hickey and S. Trebst, *Nature Communications* **10**, 530 (2019).
- [16] H.-C. Jiang, Z.-C. Gu, X.-L. Qi, and S. Trebst, *Phys. Rev. B* **83**, 245104 (2011).
- [17] J. c. v. Chaloupka, G. Jackeli, and G. Khaliullin, *Phys. Rev. Lett.* **110**, 097204 (2013).
- [18] J. Osorio Iregui, P. Corboz, and M. Troyer, *Phys. Rev. B* **90**, 195102 (2014).
- [19] J. G. Rau, E. K.-H. Lee, and H.-Y. Kee, *Phys. Rev. Lett.* **112**, 077204 (2014).
- [20] K. Shinjo, S. Sota, and T. Tohyama, *Phys. Rev. B* **91**, 054401 (2015).
- [21] M. Gohlke, R. Verresen, R. Moessner, and F. Pollmann, *Phys. Rev. Lett.* **119**, 157203 (2017).
- [22] D. Gotfryd, J. Rusnačko, K. Wohlfeld, G. Jackeli, J. c. v. Chaloupka, and A. M. Oleś, *Phys. Rev. B* **95**, 024426 (2017).
- [23] M. Kurita, Y. Yamaji, S. Morita, and M. Imada, *Phys. Rev. B* **92**, 035122 (2015).
- [24] P. A. Mishchenko, Y. Kato, and Y. Motome, *Physical Review D* **104**, 10.1103/physrevd.104.074517 (2021).
- [25] S.-S. Zhang, G. B. Halász, and C. D. Batista, *Nat Commun* **13**, 399 (2022).
- [26] A. C. Y. Li, M. S. Alam, T. Iadecola, A. Jahin, D. M. Kurcuoglu, R. Li, P. P. Orth, A. B. Özgüler, G. N. Perdue, and N. M. Tubman, Benchmarking variational quantum eigensolvers for the square-octagon-lattice kitaev model (2021), [arXiv:2108.13375 \[quant-ph\]](https://arxiv.org/abs/2108.13375).
- [27] T. A. Bespalova and O. Kyriienko, Quantum simulation and ground state preparation for the honeycomb kitaev model (2021), [arXiv:2109.13883 \[quant-ph\]](https://arxiv.org/abs/2109.13883).
- [28] X. Xiao, J. K. Freericks, and A. F. Kemper, *Quantum* **5**, 553 (2021).
- [29] J. T. Seeley, M. J. Richard, and P. J. Love, *The Journal of Chemical Physics* **137**, 224109 (2012), [arXiv: 1208.5986](https://arxiv.org/abs/1208.5986).
- [30] P. Jordan and E. Wigner, *Zeitschrift f r Physik* **47**, 631–651 (1928).
- [31] S. B. Bravyi and A. Y. Kitaev, *Annals of Physics* **298**, 210–226 (2002).
- [32] F. Verstraete and J. I. Cirac, *Journal of Statistical Mechanics: Theory and Experiment* **2005**, P09012–P09012 (2005).
- [33] N. Moll, A. Fuhrer, P. Staar, and I. Tavernelli, *Journal of Physics A: Mathematical and Theoretical* **49**, 295301 (2016).
- [34] J. D. Whitfield, V. Havlíček, and M. Troyer, *Physical Review A* **94**, 10.1103/physreva.94.030301 (2016).
- [35] J. Preskill, *Quantum* **2**, 79 (2018).
- [36] A. Peruzzo, J. McClean, P. Shadbolt, M.-H. Yung, X.-Q. Zhou, P. J. Love, A. Aspuru-Guzik, and J. L. O’Brien, *Nature Communications* **5**, 4213 (2014).
- [37] M. Cerezo, A. Arrasmith, R. Babbush, S. C. Benjamin, S. Endo, K. Fujii, J. R. McClean, K. Mitarai, X. Yuan, L. Cincio, and P. J. Coles, Variational quantum algorithms (2020), [arXiv:2012.09265 \[quant-ph\]](https://arxiv.org/abs/2012.09265).
- [38] P. J. O’Malley, R. Babbush, I. D. Kivlichan, J. Romero, J. R. McClean, R. Barends, J. Kelly, P. Roushan, A. Tranter, N. Ding, *et al.*, **6**, 031007 (2016).
- [39] A. Kandala, A. Mezzacapo, K. Temme, M. Takita, M. Brink, J. M. Chow, and J. M. Gambetta, *Nature* **549**, 242 (2017).
- [40] C. Hempel, C. Maier, J. Romero, J. McClean, T. Monz, H. Shen, P. Jurcevic, B. P. Lanyon, P. Love, R. Babbush, A. Aspuru-Guzik, R. Blatt, and C. F. Roos, *Phys. Rev. X* **8**, 031022 (2018).
- [41] A. J. McCaskey, Z. P. Parks, J. Jakowski, S. V. Moore, T. D. Morris, T. S. Humble, and R. C. Pooser, **5**, 99 (2019).
- [42] F. Arute, K. Arya, R. Babbush, D. Bacon, J. C. Bardin, R. Barends, S. Boixo, M. Broughton, B. B. Buckley, D. A. Buell, B. Burkett, N. Bushnell, Y. Chen, Z. Chen, B. Chiaro, R. Collins, W. Courtney, S. Demura, A. Dunsworth, D. Eppens, E. Farhi, A. Fowler, B. Foxen, C. Gidney, M. Giustina, R. Graff, S. Habegger, M. P. Harrigan, A. Ho, S. Hong, T. Huang, W. J. Huggins, L. Ioffe, S. V. Isakov, E. Jeffrey, Z. Jiang, C. Jones, D. Kafri, K. Kechedzhi, J. Kelly, S. Kim, P. V. Klimov, A. Korotkov, F. Kostritsa, D. Landhuis, P. Laptev, M. Lindmark, E. Lucero, O. Martin, J. M. Martinis, J. R. McClean, M. McEwen, A. Megrant, X. Mi, M. Mohseni, W. Mruczkiewicz, J. Mutus, O. Naaman, M. Neeley, C. Neill, H. Neven, M. Y. Niu, T. E. O’Brien, E. Ostby, A. Petukhov, H. Putterman, C. Quintana, P. Roushan, N. C. Rubin, D. Sank, K. J. Satzinger, V. Smelyanskiy, D. Strain, K. J. Sung, M. Szalay, T. Y. Takeshita, A. Vainsencher, T. White, N. Wiebe, Z. J. Yao, P. Yeh, and A. Zaleman, [arXiv:2004.04174 \[physics, physics:quant-ph\]](https://arxiv.org/abs/2004.04174) (2020), [arXiv: 2004.04174](https://arxiv.org/abs/2004.04174).
- [43] E. Farhi, J. Goldstone, S. Gutmann, and M. Sipser, Quantum computation by adiabatic evolution (2000), [arXiv:quant-ph/0001106 \[quant-ph\]](https://arxiv.org/abs/quant-ph/0001106).
- [44] M. Motta, C. Sun, A. T. K. Tan, M. J. O’Rourke, E. Ye, A. J. Minnich, F. G. S. L. Brandão, and G. K.-L. Chan, *Nature Physics* **16**, 205–210 (2019).
- [45] E. H. Lieb, *Physical Review Letters* **73**, 2158–2161 (1994).
- [46] D. Wecker, M. B. Hastings, and M. Troyer, *Phys. Rev. A* **92**, 042303 (2015).
- [47] R. Wiersema, C. Zhou, Y. de Sereville, J. F. Carrasquilla, Y. B. Kim, and H. Yuen, *PRX Quantum* **1**, 020319 (2020).
- [48] H. Xu and J. M. Taylor, Developing a robust approach to implementing non-abelian anyons and topological quantum computing in a modified kitaev honeycomb lattice model (2011), [arXiv:1104.0024 \[cond-mat.str-el\]](https://arxiv.org/abs/1104.0024).

- [49] S. D. Sarma, M. Freedman, and C. Nayak, npj Quantum Information **1**, [10.1038/npjqi.2015.1](https://doi.org/10.1038/npjqi.2015.1) (2015).
- [50] O. Crawford, B. v. Straaten, D. Wang, T. Parks, E. Campbell, and S. Brierley, *Quantum* **5**, 385 (2021).
- [51] T.-C. Yen, V. Verteletskyi, and A. F. Izmaylov, Measuring all compatible operators in one series of a single-qubit measurements using unitary transformations (2020), [arXiv:1907.09386](https://arxiv.org/abs/1907.09386) [quant-ph].
- [52] A. Jena, S. Genin, and M. Mosca, Pauli partitioning with respect to gate sets (2019), [arXiv:1907.07859](https://arxiv.org/abs/1907.07859) [quant-ph].
- [53] V. Verteletskyi, T.-C. Yen, and A. F. Izmaylov, *The Journal of Chemical Physics* **152**, 124114 (2020).
- [54] A. Zhao, A. Tranter, W. M. Kirby, S. F. Ung, A. Miyake, and P. J. Love, *Physical Review A* **101**, [10.1103/physreva.101.062322](https://doi.org/10.1103/physreva.101.062322) (2020).